PAPER

Check for updates

Synthesis and reactivity of titanium 'POCOP' pincer complexes†

Leah Webster,[a] Tobias Krämer [ID][b] and F. Mark Chadwick [ID] *[a]

The 'POCOP' pincer ligand, [2,6-(OPR$_2$)$_2$C$_6$H$_3$], has been attached to titanium in both Ti(III) and Ti(IV) complexes for the first time. Using a lithium-halogen exchange route [2,6-(OPR$_2$)$_2$C$_6$H$_3$]Li (**[^{R}POCOP]Li**) can be synthesised. Both the *iso*-propyl and *tert*-butyl derivatives can be made, but only the latter isolated. These can be reacted with the Ti(III) and Ti(IV) synthons to make a range of [POCOP]TiCl$_x$ species. In the presence of Ti(IV), THF and **[^{R}POCOP]Li**, an unprecedented ligand rearrangement occurs. (^{tBu}POCOP)TiCl$_2$, **1**, can be derivatised with alkylating agents to make bis-methyl, phenyl and neopentyl complexes. The last of these can activate H$_2$ to make a rare example of a titanium chlorohydride, with the metal pincer fragment staying attached. EPR has been used to characterise the paramagnetic complexes and locate their electron spins, which is further validated with DFT calculations. This opens the door for this archetypical pincer ligand to be used with early transition metals.

Introduction

Since their initial discovery by Shaw in 1976 pincer complexes have held a privileged position in organometallic chemistry.[1–3] Pincer complexes are widely applied in catalysis for example in hydrogenations using first-row transition metals,[4] iridium and ruthenium catalysed alkane dehydrogenation,[5] and cross-coupling reactivity.[6] Pincer ligands also support interesting reactivity, for example acting as a two-electron sink to augment reactivity.[7] Of the many different pincer ligands developed some of the most recognisable are those of the ^{R}PCP and ^{R}POCOP design, where a central arene is flanked by two phosphines connected *via* a methylene group or an oxygen atom respectively (^{R}PCP = 2,6-(CH$_2$PR$_2$)$_2$C$_6$H$_3$; ^{R}POCOP = 2,6-(OPR$_2$)$_2$C$_6$H$_3$).

The ^{R}PCP ligand is the progenitor of pincer ligands. It, and its close cousin ^{R}POCOP have been extensively used with late transition metals. The ease of changing the phosphine and arene substituents has resulted in these ligands being adopted in a multitude of challenging reactivity.[8] For example Ir ^{R}POCOP complexes have been used in tandem with olefin metathesis catalysts to perform alkane metathesis,[9] and have been able to support single-crystal to single-crystal ligand exchange.[10] However to date there are only two reports of the ^{R}POCOP motif being used with early transition metals.[11,12]

The origin of this scarcity is that the traditional route to these complexes relies on the oxidative addition of a strong C–H bond, which is disfavoured for early transition metals (both because of the relatively weak bonds formed, and the lack of suitable synthons in an N-2 oxidation state).

However early transition metal pincer complexes are enjoying a renaissance.[13] Pioneered by Fryzuk's work on aliphatic 'PNP' pincer complexes,[14] more recently others have taken up the baton making early transition metal pincer complexes capable of activating small molecules (*e.g.* N$_2$, CH$_4$) in interesting reactivity.[15–24] An issue with these systems is that they can be challenging to derivatise in order to tune the steric and electronic profile of the pincer ligand. Of particular interest would be the isolation of early transition metal hydrides. These have been invoked as intermediates in the activation of N$_2$ and isolable titanium monohydrides are able to C–H activate arenes.[25–27] Arguably even rarer than isolable titanium hydrides are titanium chlorohydrides, which are 'often invoked but never (*sic.*) observed'.[28] Though this quote refers to titanocene chlorohydride there are still only two structurally characterised titanium chlorohydrides (excluding those where the hydride is supported by another element, *e.g.* boron).[29,30]

Herein we report the selective synthesis of ^{R}POCOP Titanium complexes. We demonstrate ligand platforms with different steric profiles and binding to the metal in multiple oxidation states (with divergent chemistries). We have taken one of these synthons further onwards, derivatising it to make a number or alkyl and aryl Ti(^{R}POCOP) complexes. One of these is reacted with dihydrogen to form a rare example of an isolable Ti chlorohydride, displaying the ^{R}POCOP ligands' ability to support interesting reactivity from the metal centre.

[a] Department of Chemistry, Molecular Sciences Research Hub, Imperial College London, 82 Wood Lane, W12 0BZ, UK. E-mail: m.chadwick@imperial.ac.uk
[b] Department of Chemistry, Maynooth University, Maynooth, Co. Kildare, Ireland
†Electronic supplementary information (ESI) available. CCDC 2204753–2204761. For ESI and crystallographic data in CIF or other electronic format see DOI: https://doi.org/10.1039/d2dt03291k
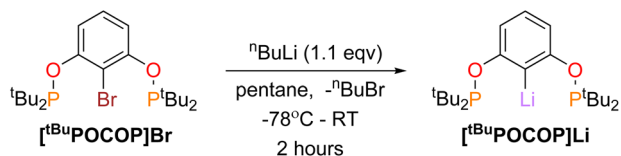
Results and discussion

Synthesis of titanium ^{R}POCOP complexes was achieved *via* the salt metathesis reaction of the lithium salt of the ^{R}POCOP ligand and either TiCl$_3$(THF)$_3$ or TiCl$_4$. A similar method from the iodo-^{R}POCOP compound has been described, however the lithiated material was not isolated nor characterised.[31,32] [^{tBu}**POCOP]Li** (^{R}POCOP = 2,6-(OPR$_2$)C$_6$H$_3$) was isolated *via* the lithium halogen exchange reaction of (^{tBu}POCOP)Br with a slight excess of ^{n}BuLi (Scheme 1, yield 99%).

[^{tBu}**POCOP]Li** can be stored at −40 °C in an inert atmosphere as a colourless solid for over two months with no degradation. [^{tBu}**POCOP]Li** is extremely moisture-sensitive and exposure to water leads to intractable contamination by (^{tBu}POCOP)H. [^{tBu}**POCOP]Li** is extremely soluble in hydrocarbon solvents, including aliphatic solvents. Crystals of [^{tBu}**POCOP]Li** suitable for X-ray diffraction were grown from slow evaporation of a pentane solution (Fig. 1).

Organolithium compounds aggregate in the solution phase (and indeed in the solid and gaseous phase) to varying degrees.[33] There are only a couple of other examples of a lithium 'PCP' complexes.[34,35] [^{tBu}**POCOP]Li** has a similar structure to the related [^{Me}PCP]Li complex.[35] The dimeric structure of [^{tBu}**POCOP]Li** is retained in non-donor solvents at room temperature. This is demonstrated by a quintet resonance in the ^{7}Li{^{1}H} NMR spectrum, though some fluxionality must be present to allow the Li centres to couple equally to all four phosphorus atoms in the dimer. Such fluxionality in pincer complexes has precedence.[35,36]

Synthesis of Titanium(III) POCOP Chloride, (^{tBu}POCOP)TiCl$_2$, (1)

The synthesis of (^{tBu}POCOP)TiCl$_2$, (**1**) in pentane (Scheme 2) yielded an electric blue solution from which **1** was isolated as a light blue solid. A similar synthesis has recently been reported, however with minimal characterising data.[12] An improved crystalline yield can be achieved by recrystallising **1** from cyclopentane (59%).

Evan's NMR of **1** determined an μ_{eff} value of 1.86 μ_B, corresponding to one unpaired electron on the titanium centre, which was confirmed by the DFT-calculated spin density (see ESI†). Unfortunately, due to the paramagnetic nature of the complex, only broad resonances were observed in the ^{1}H NMR spectrum (see ESI†) and no resonances were observed in the ^{31}P{^{1}H} NMR spectrum.

The presence of a titanium(III) metal centre was further confirmed by X-Band CW EPR of **1** (Fig. 2). The room temperature EPR signal is a triplet with a g_{iso} value of 1.9665 and isotropic hyperfine coupling value, a_0 of 2.31 mT, This is representative of a single unpaired electron centred on the titanium atom coupled to two equivalent phosphorus (I = 1/2) nuclei.[15]

Synthesis of titanium(IV) POCOP chlorides, (^{R}POCOP)TiCl$_3$, (2)

The reaction of [^{tBu}**POCOP]Li** and TiCl$_4$ in pentane (Scheme 3) yields (^{tBu}POCOP)TiCl$_3$, **2**, as a red solid in 57% yield. Single crystals suitable for X-ray diffraction studies were grown from a saturated hexane solution cooled to −40 °C. **2** is the Ti(IV) analogous complex of **1**.

The solid-state structure of **2** (Fig. 3) shows titanium in an extremely distorted octahedral geometry, with the sum of the angles around the equatorial plane (featuring the POCOP ligand and Cl(2)) being 364.46(4)° but the axial Cl(1)–Ti(1)–Cl(3) angle being only 143.16(4)°. The origin of this distortion appears to be due to a second-order Jahn Teller effect, but a more comprehensive theoretical analysis is currently beyond the scope of this paper. Generally the Ti(1)–X bond lengths show a small increase when compared to **1**, presumably due to the increased steric encumbrance in **2**.

The ^{1}H NMR spectrum shows the characteristic doublet resonance for the P^{t}Bu$_2$ groups (1.41 ppm, $^{2}J_{(H-P)}$ 13 Hz) and

Scheme 1 Synthesis of [^{tBu}**POCOP]Li**.
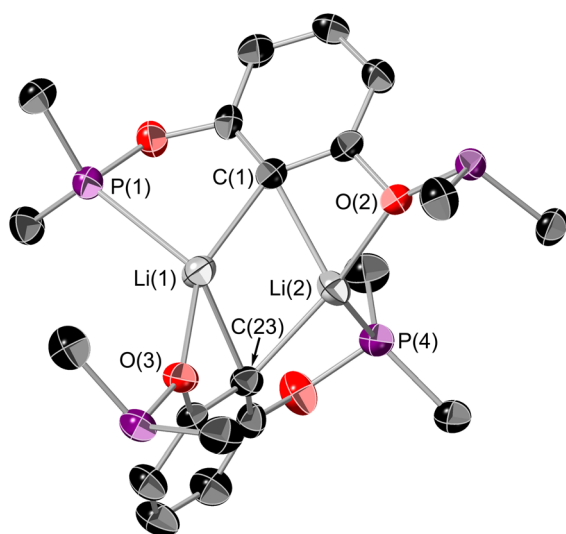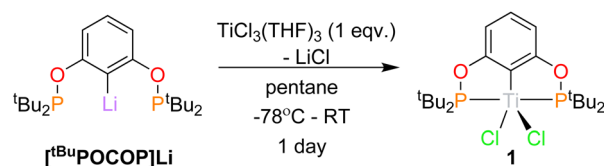

Fig. 1 ORTEP plot of [^{tBu}**POCOP]Li**. Thermal ellipsoids at 50% probability, hydrogens omitted for clarity. ^{t}Bu groups on phosphines only have the central carbon shown for clarity. Colour key: black (carbon); purple (phosphorus), red (oxygen), grey (lithium). Selected bond lengths (Å): Li(1)−C(1) 2.197(11), Li(1)−C(23) 2.264(11), Li(1)−O(3) 2.164(10), Li(1)−P(1) 2.614(10), Li(2)−C(1) 2.234(11), Li(2)−C(23) 2.192(11), Li(2)−O(2) 2.116(9), Li(2)−P(4) 2.544(10).
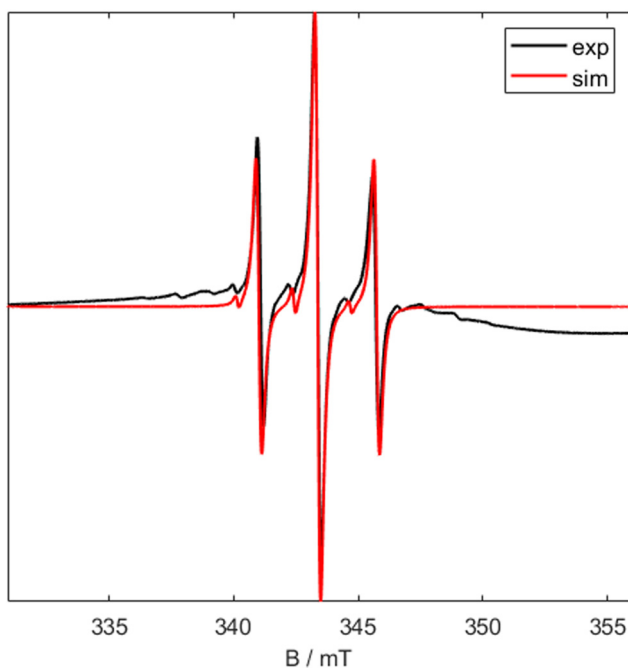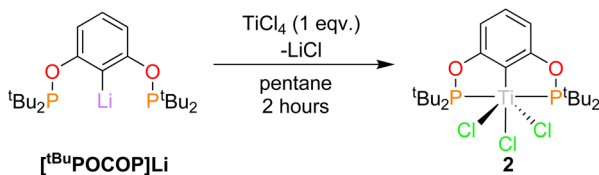

Scheme 2 Synthesis of **1**.

Fig. 2 X Band CW EPR spectrum of **1** at room temperature. Black shows experimental data and red shows simulated data (g_{iso} = 1.9665, a_0 = 2.31 mT).
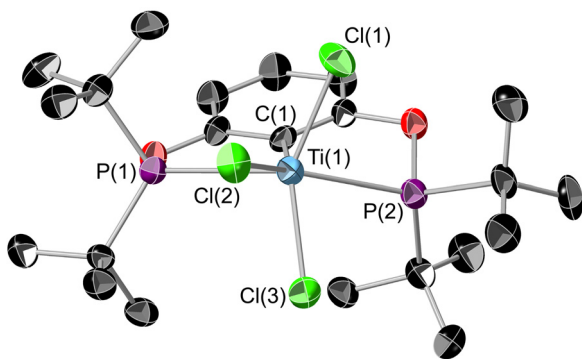

Scheme 3 Synthesis of **2**.

Fig. 3 ORTEP plot of **2**. Thermal ellipsoids at 50% probability, hydrogens omitted for clarity. Colour key: sky blue (titanium), black (carbon); purple (phosphorus), red (oxygen), green (chlorine). Selected bond lengths (Å) and bond angles (°): Ti−C(1) 2.2081(11), Ti(1)−P(1) 2.6133 (11), Ti(1)−P(2) 2.6330(11), Ti(1)−Cl(1) 2.2643(11), Ti(1)−Cl(2) 2.3831(10), Ti (1)−Cl(3) 2.3006(10); Σ equatorial angles: 364.46(4) [C(1)−Ti(1)−P(1) 71.80(4), C(1)−Ti(1)−P(2) 68.64(4), P(1)−Ti(1)−Cl(2) 79.55(3), P(2)−Ti(1)−Cl(2) 144.47(4)], Cl(1)−Ti(1)−Cl(3) 143.16(4).

the $^{31}P\{^1H\}$ NMR spectrum shows a single resonance at 187.6 ppm, roughly 30 ppm downfield from the free protonated ligand, (^{tBu}POCOP)H at 153.1 ppm.[37]

Unexpectedly, targeting **2** using [^{tBu}**POCOP**]**Li** and a different titanium synthon, TiCl$_4$(THF)$_2$, instead promoted ligand rearrangement, yielding (κ^2-O,P-(1-O-2-P^{t}Bu$_2$-3-(OP^{t}Bu$_2$)-C$_6$H$_3$)$_2$TiCl$_2$, **3** (Scheme 4). This structure sees one of the O–P bonds cleaved and the phosphine group migrating to the original *ipso* carbon. Two rearranged ligands bind to the single titanium metal centre. This is the first example of such a rearrangement of the POCOP ligand.

THF is required for this rearrangement to occur – conducting the reaction in toluene or diethyl ether does not produce either **2** or **3**. **2** cannot be converted to **3** despite heating in THF and excess [^{tBu}**POCOP**]**Li**. Heating [^{tBu}**POCOP**]**Li** in THF in the absence of stoichiometric titanium does not induce ligand rearrangement. **3** is still exclusively the only observable product even with a strict 1 : 1 equivalence of TiCl$_4$(THF)$_2$ and [^{tBu}**POCOP**]**Li**. This rearrangement is curiously not seen with TiCl$_3$(THF)$_3$. This appears to be an unique rearrangement in the presence of both Ti(IV) and THF.

The rearrangement is clearly seen in the ^1H and $^{31}P\{^1H\}$ NMR spectra with two resonances observed corresponding to the *tert*-butyl protons; one ^{t}Bu ^1H resonance still observed as a doublet at 1.10 ppm ($^2J_{H–P}$ = 12 Hz) whilst the other observed as a broad singlet (1.76 ppm). The $^{31}P\{^1H\}$ NMR spectrum also displays two resonances which integrate 1 : 1, one at 159.0 ppm, which is a similar chemical shift to the free protonated ligand,[37] whilst the other is upfield at 78.2 ppm. These are assigned to the free and ligating phosphine respectively.

Single crystals of **3**, suitable for X-ray diffraction, could be grown by cooling a saturated hexane solution to −40 °C (Fig. S1†). The poor quality of the X-ray data means detailed structural analysis is not appropriate, however the titanium clearly adopts an approximately octahedral geometry, as demonstrated by the P(1)–Ti(1)–P(3) and Cl(1)–Ti(1)–Cl(2) angles (178.4(2)° and 95.3(2)° respectively). The deviation from ideal octahedral geometry arises due to the constraint of the P and O being 1,2-substituted on the arene ring, thus pulling the oxygen away (P(1)–Ti(1)–O(1) 71.3(4)°). This is also presumably the cause for the slight lengthening of the Ti–P bonds as compared with **2**.

Only a single stereoisomer of this product is observed, with the two phosphine groups trans to each other and the chloride and oxo groups in *cis* geometries. This is demonstrated by only one ligating ^{31}P resonance observed in the $^{31}P\{^1H\}$ NMR spectrum and no P–P coupling as the P centres are equivalent. The isomer shown in Scheme 4 has been determined to be the lowest energy isomer by DFT, with all possible isomers and their relative energies shown in Fig. 4.

To explore the influence of sterics within the ligand, and prove the broader applicability of this route to tuneable ligands, the *iso*-propyl derivative was also targeted. It was found ^{t}BuLi was needed to affect the lithium-halogen exchange – [^{iPr}**POCOP**]**Li** is an off-white oil, and could not be isolated. However it could be made *in situ* and used directly onwards in
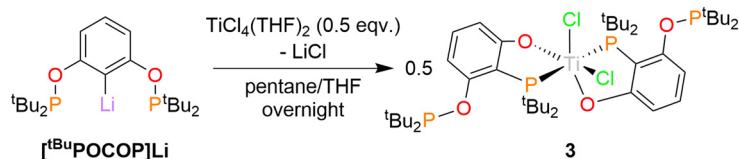
Scheme 4 Synthesis of **3**.
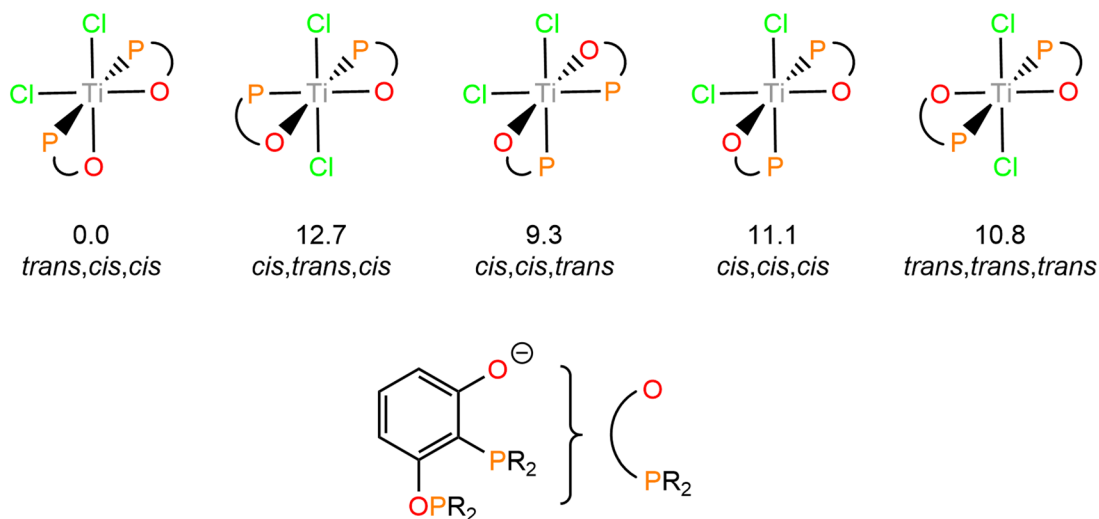
Fig. 4 Isomers of **3** and their relative Gibbs Free Energies (in kcal mol^{-1}) calculated at the BP86-D3(BJ)/def2-TZVP/def2-SVP level of theory.

reaction with TiCl$_4$ in pentane. This yielded dimeric $\{(^{iPr}POCOP)TiCl_2(\mu\text{-}Cl)\}_2$ (**4**, Scheme 5).

Single crystals of **4** suitable for X-ray diffraction can be grown from a saturated hexane solution cooled to −40 °C (Fig. 5). The geometry around the titanium is a near-perfect pentagonal bipyramid (Σ equatorial angles 360.89(5)°). The structural parameters are in line with similar motifs,[38] for example the Ti–Cl distance for the terminal Cl is nearly identical to that found in **2**.

The origin of the structural difference between **2** and **4** arises due to the reduction of steric encumbrance due to the ligands. The dimeric structure is 15 kcal mol^{-1} more favoured than the monomeric structure for **4**. However making the substituents ^{t}Bu rather than ^{i}Pr reverses this, making the mono-
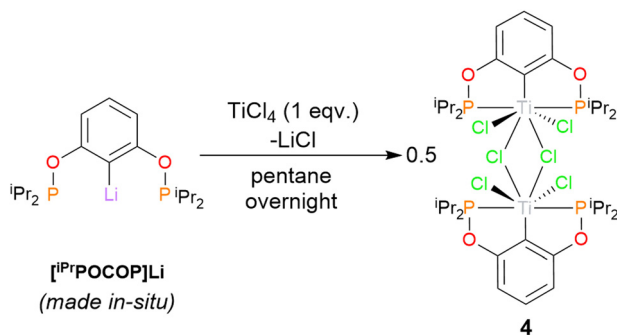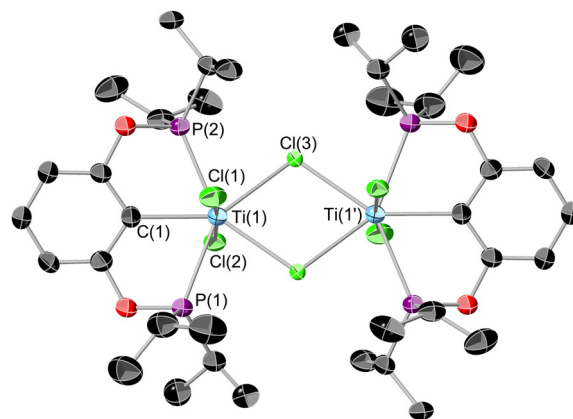

Fig. 5 ORTEP plot of **4**. Thermal ellipsoids at 50% probability, hydrogens omitted for clarity. Selected bond lengths (Å) and bond angles (°): Ti(1)−Cl(1) 2.293(1), Ti(1)−Cl(2) 2.336(1), Ti(1)−Cl(3) 2.587(1), Ti(1)−P(1) 2.578(1), Ti(1)−P(2) 2.587(1), Ti(1)−C(1) 2.252(4), Ti(1)−Ti(1') 4.116(1), Σ equatorial angles 360.89(5), Cl(1)−Ti(1)−Cl(2) 174.05(5).

meric form 1 kcal mol^{-1} more stable than the dimer. There is still a small steric clash in the *iso*-propyl derivative when compared to a simple methylated model (see ESI†)

Derivatisations of (^{tBu}POCOP)TiCl$_2$

With a high-yielding synthesis of **1** devised alkylation and arylation experiments were undertaken. Attempts at alkylating **2** with Grignard and alkyl lithium reagents resulted in reduction.
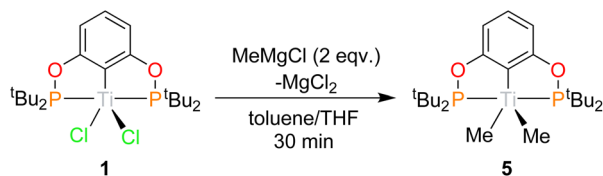
Scheme 5 Synthesis of **4**.

Paper

Methyl

1 can be reacted with two equivalents of MeMgCl resulting in an immediate colour change from blue to teal, forming (^{tBu}POCOP)TiMe$_2$ (**5**, Scheme 6). To date, there has been no observation of a monomethylated complex (^{tBu}POCOP)TiMeCl. Teal crystals suitable for X-ray diffraction studies can be grown from a concentrated pentane solution cooled to −40 °C (Fig. 6). The geometry around the titanium centre remained unchanged from the starting material as a square based pyramid, with a τ_5 parameter of 0.017 and C(1) determined to be the axial ligand.[39]

The Ti–P bond lengths are slightly elongated in **5** when compared to **1**. The Ti–Me distances are comparable to other Ti pincer dimethyl complexes.[19,40] **5** is paramagnetic with a μ_{eff} = 2.03μ_B (Evan's method). Fig. 7 shows the X band CW EPR of **5** measured at 298 K.

The experimental spectrum in Fig. 7 can be simulated as a triplet of septets (g_{iso} = 1.970; a_0 = 2.251 mT, 0.642 mT). This arises due to coupling of the electron to the two ^{31}P nuclei and slightly weaker coupling to the six ^{1}H attached to the methyl groups. This implies that the SOMO is primarily positioned on the titanium centre (implied by the g value) but has significant character on both the phosphorus and methyl ligands.

Phenyl

When **1** was reacted with PhMgCl, only the monosubstituted product was isolated, (^{tBu}POCOP)TiPhCl (**6**), even if excess PhMgCl is used or the reaction is heated overnight (Scheme 7). Use of PhMgBr on one occasion resulted in halogen exchange resulting in (^{tBu}POCOP)TiPhBr (see ESI†). Single crystals of **6**
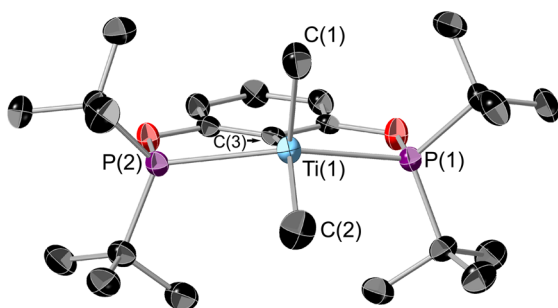
Scheme 6 Synthesis of **5**.

Fig. 6 ORTEP plot of **5**. Thermal ellipsoids at 50% probability, hydrogens omitted for clarity. Selected bond lengths (Å) and bond angles (°): Ti(1)–P(1) 2.6243(9), Ti(1)–P(2) 2.6180(9), Ti(1)–C(1) 2.138(4), Ti(1)–C(2) 2.143(4), Ti(1)–C(3) 2.241(3), P(1)–Ti(1)–P(2) 141.44(3), C(2)–Ti(1)–C(3) 140.53(14).
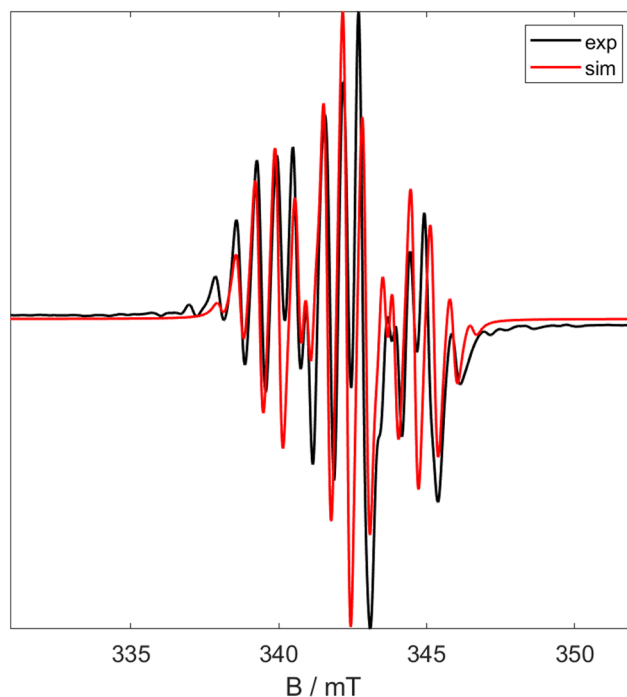
Fig. 7 X Band CW EPR spectra of **5** at room temperature. Black shows experimental data and red shows simulated data (g_{iso} = 1.970, a_0 = 2.25 mT, 0.64 mT).

suitable for X-ray diffraction studies could be grown from cooling a concentrated pentane solution of **6** to −40 °C (Fig. 8).

The geometry around the titanium centre remained unchanged from the starting material as square based pyramid, with a τ_5 parameter of 0.011 and the phenyl ring in the axial position. The plane of the phenyl ring is perpendicular to the POCOP aryl ring. Interestingly this is only the second example of a crystallographically characterised 'TiPhCl' fragment with an unsubstituted phenyl ring.[40]

The room temperature X band CW EPR spectrum of **6** (see ESI, Fig. S4†) consistently appeared to have two signals, one major (60%, g_{iso} = 1.9665, a_0 = 2.26 mT) and one minor (40%, g_{iso} = 1.9720, a_0 = 2.24 mT). These apparent two signals occur even if excess PhMgCl is used in the synthesis and are both due to **6** (see later Q-band EPR studies of (^{tBu}POCOP)TiNpCl, **7**). The magnetic moment was measured by Evan's method (μ_{eff} = 2.08μ_B). These data imply there is a single unpaired electron that is almost entirely located on the titanium centre with some coupling to the phosphorus atoms.

Neopentyl

1 can also be derivatised using organolithiums, and the addition of 1 equivalence of neopentyl lithium yields (^{tBu}POCOP)TiClNp (**7**) as dark green crystals in 63% yield (Scheme 8). Similarly to **6**, substitution of two chloride ligands for neopentyl fragments does not occur, even when using excess neopentyl lithium and forcing conditions. Single crystals suitable for X-ray crystallography can be grown from a saturated pentane solution cooled to −40 °C (Fig. 9).
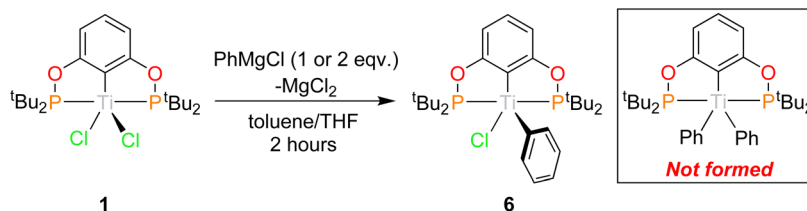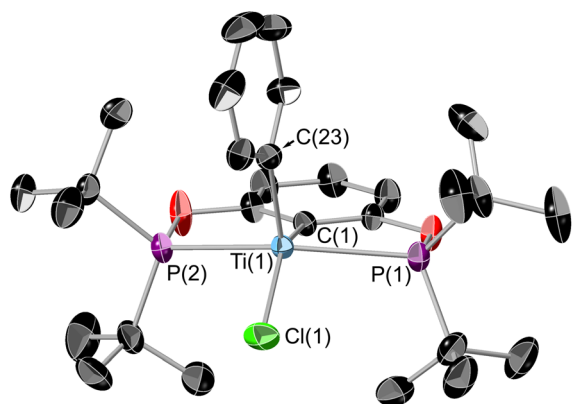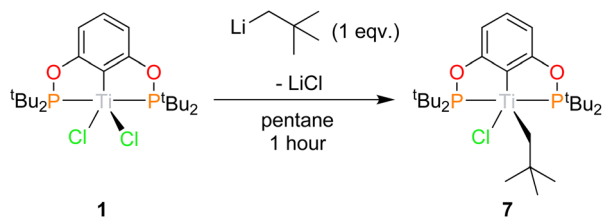
Scheme 7 Synthetic route to (^{tBu}POCOP)TiPhCl.

Fig. 8 ORTEP plot of **6**. Thermal ellipsoids at 50% probability, hydrogens omitted for clarity. Selected bond lengths (Å) and bond angles (°): Ti(1)–P(1) 2.6109(6), Ti(1)–P(2) 2.6109(6), Ti(1)–C(1) 2.2129(19), Ti(1)–C(23) 2.100(2), Ti(1)–Cl(1) 2.3157(6), P(1)–Ti(1)–P(2) 143.72(2), C(1)–Ti(1)–Cl(1) 144.36(5).

Scheme 8 Synthesis of **7**.

The geometry around the titanium centre is still a square based pyramid, however significantly more distorted than **1** ($\tau_5 = 0.265$ for **7**). The neopentyl fragment is remarkably distorted towards linerarity around C1 (Ti(1)–C(1)–C(2) = 156.3(5)°), such a distortion could arise from some form of agostic interactions with the C–H bonds around C(1). This interaction must be somewhat fluxional however since no coupling to these protons is observed in the room-temperature solution EPR (see ESI, Fig. S5†). The single crystal X-ray data was of insufficient quality to refine the H-atom positions. The optimised geometry of **7** employing the BP86-D3 functional allows for a more detailed analysis of the interaction between the neopentyl fragment and titanium. The bond metrics associated with the crystallographic structure are reproduced very well. The computed Ti⋯H(1) distance of 2.04 Å is signifi-

cantly shorter than Ti⋯H(2) with 2.44 Å. Additionally, both C(1)–H bonds are somewhat elongated with respect to the remaining C–H bonds (1.11 Å), although distances of 1.14 Å and 1.12 Å for C(1)–H(1) and C(1)–H(2), respectively, imply that this effect is more pronounced for the former (Fig. S45†). The weakening of these bonds is also reflected in their stretching frequencies which are red-shifted to $\nu_{C(1)H(1)} = 2689$ cm^{-1} and $\nu_{C(1)H(2)} = 2888$ cm^{-1}, while the other C–H bonds show symmetric and antisymmetric modes at around 3087 cm^{-1} and 2959 cm^{-1}, respectively. These data are diagnostic of α-agostic interactions between Ti and the C(1)H$_2$ group, where exchange of the symmetry-equivalent hydrogen atoms would imply a degree of fluxionality. This is further validated by NBO and QTAIM analyses of the computed electron density (see Fig. S46 and S47†). For the former, several contributions to $\sigma_{CH} \rightarrow d_{Ti}$ donor/acceptor interactions can be identified, with the leading interactions stabilising the structure by ~7–13 kcal mol^{-1}, considering both α- and β-spin manifolds. The topology analysis reveals reduced QTAIM parameters associated with the bond critical points (BCPs) of C(1)–H(1) ($\rho(r) = 0.245$ au; $\nabla^2\rho(r) = -0.734$ au) and C(1)–H(2) ($\rho(r) = 0.257$ au; $\nabla\rho^2(r) = -0.835$ au), diagnostic of weakened bonds due to their interaction with the Ti centre. No BCP for the Ti⋯H interaction could be located, however, the complete absence of BCPs and associated bond paths in these types of systems is not uncommon and is not considered a requirement for agostic interactions.[41,42]

Similarly to **1** and **6**, **7** only displays a triplet in the EPR, indicating the unpaired electron is centred on the metal centre (major component $g = 1.9665$) but couples to the two ^{31}P nuclei ($a_0 = 2.20$ mT). Also similarly to **6** the X band spectrum shows a minor component. In order to deduce whether this is due to an impurity measurements were carried out using Q band radiation. The resultant spectrum is shown in Fig. 10 and shows the signal has collapsed to a simple triplet. This shows that the minor component in the X band EPR is due to coupling and not due to an impurity. The effective magnetic moment ($\mu_{eff} = 1.75\mu_B$) was measured using Evan's method and corresponds to a single unpaired electron.

Hydrogen activation studies

Having demonstrated the ability of the '(^{tBu}POCOP)Ti' platform to allow for derivatisation the possibility that these complexes could be used to activate small molecules was explored. For the '(^RPOCOP)Ti' to be useful in reactivity it is imperative that the pincer-metal fragment remains intact in reactive con-
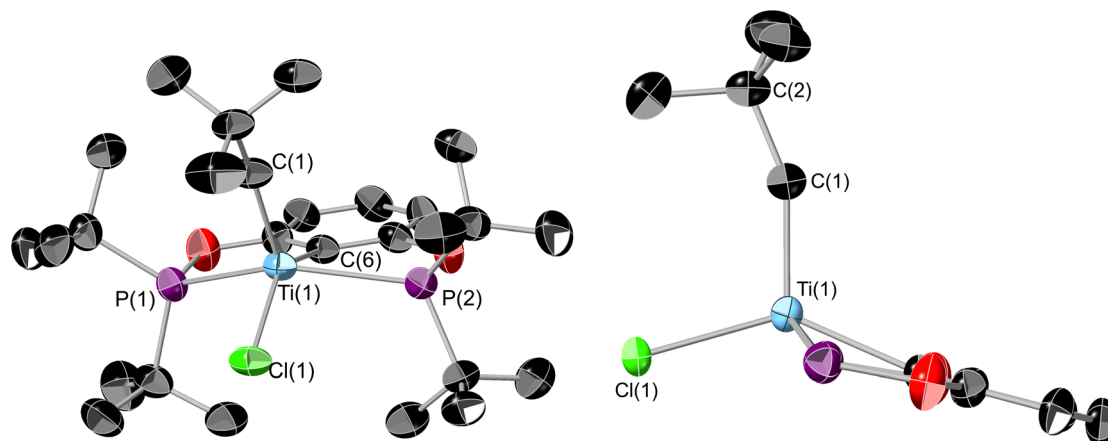
Fig. 9 Two ORTEP plots of **7**. Thermal ellipsoids at 50% probability, hydrogens omitted for clarity. The phosphine *tert*-butyl groups are omitted from the side-on view. Selected bond lengths (Å) and bond angles (°): Ti(1)−P(1) 2.6223(17), Ti(1)−P(2) 2.6232(17), Ti(1)−C(1) 2.033(6), Ti(1)−C(6) 2.222 (5), Ti(1)−Cl(1) 2.3799(14), P(1)−Ti(1)−P(2) 139.03(6), C(6)−Ti(1)−Cl(1) 140.40(15), Ti(1)−C(1)−C(2) 156.3(5).
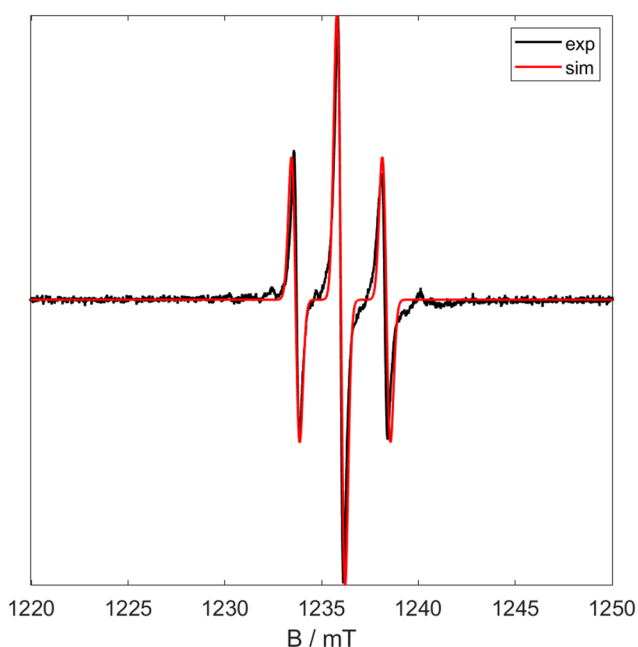

Fig. 10 Q Band CW EPR spectra of **5** at room temperature. Black shows experimental data and red shows simulated data (g_{iso} = 1.9665, a_0 = 2.30 mT).

ditions. One of the most fundamental reactions is the activation of hydrogen. When a pentane solution of **7** was charged with 1 bar of dihydrogen the solution quickly changed from green to royal purple. Single crystals X-ray diffraction studies showed this product to be $[(^{tBu}POCOP)TiCl(\mu\text{-}H)]_2$ (**8**, Scheme 9). The reaction can also proceed in the solid state, using crystalline **7** and charged with 1 bar of H_2 at room temperature. The green solid changes to purple over 10 minutes, with a loss of crystallinity.

This is a rare example of a titanium chlorohydride, with only two others being isolated and structurally characterised (excluding those that are due to another element-hydride binding to the metal centre *e.g.* BH_4^-).[29,30] Titanium chlorohydride are invoked as intermediates in a range of catalytic processes but are extremely challenging to observe.[27,28] The mechanism of the above reaction was probed by DFT calculations (see Fig. S48†). It traverses a σ-bond metathesis pathway that involves a typical four-membered kite-shaped transition state with an overall Free Energy activation barrier of 22.5 kcal mol^{-1}. Formation of monomeric $(^{tBu}POCOP)TiCl(H)$ after release of neopentane is exergonic (−9.9 kcal mol^{-1}). Subsequent dimerization of two units $(^{tBu}POCOP)TiCl(H)$ then forms **8** with an overall exergonicity of −20 kcal mol^{-1}.

Single crystals suitable for X-ray diffraction could be grown from a saturated SiMe$_4$ solution cooled to −40 °C. The resultant structure is shown in Fig. 11. The bridging hydrides could
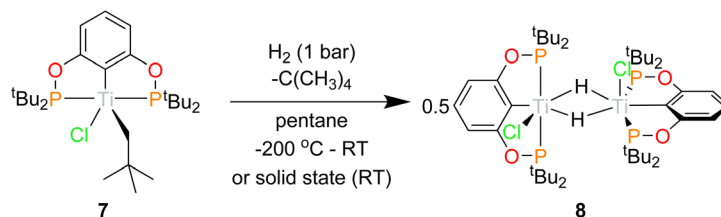
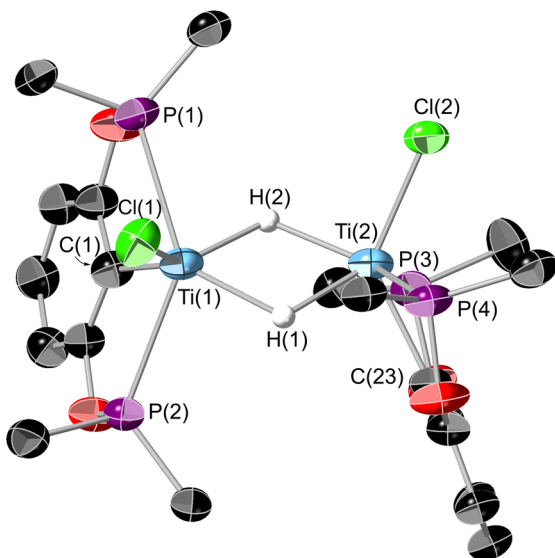**Scheme 9** Hydrogen activation by **7** to form **8**.

Fig. 11 ORTEP plot of **8**. Thermal ellipsoids at 50% probability, hydrogens (except for H(1) and H(2)) and *tert*-butyl methyl groups omitted for clarity. White sphere represent hydrogen atoms. Selected bond lengths (Å) and bond angles (°): Ti(1)–Ti(2) 3.1708(12), Ti(1)–P(1) 2.6858(13), Ti(1)–P(2) 2.6898(13), Ti(1)–C(1) 2.212(4), Ti(2)–P(3) 2.6906(13), Ti(2)–P(4) 2.6799(13), Ti(2)–C(23) 2.221(4), Ti(1)–Cl(1) 2.3157(14), Ti(2)–Cl(2) 2.3113(14), P(1)–Ti(1)–P(2) 138.03(5), C(1)–Ti(1)–Cl(1) 129.99(14), P(3)–Ti(2)–P(4) 137.77(5), C(23)–Ti(2)–Cl(2) 129.79(13). Angle between Cl(1)–Ti(1)–Ti(2) plane and Cl(2)–Ti(2)–Ti(1) plane: 72.25°.

be located on the electron density map but the data was not of sufficient quality to be able to refine their positions reliably. Interestingly these crystals were grown in a N_2 atmosphere, showing **8** to be stable in the presence of N_2. This is in contrast to previous titanium pincer hydrides.[26]

The geometry of **8** is quite distorted away from the optimal octahedron. The Ti(1)–Ti(2) distance is in the region where there could be a Ti–Ti bond,[43] however the retention of the unpaired electrons (as evidenced by the EPR spectrum, see ESI Fig. S6†), implies there is no bond present. Looking down the Ti–Ti axis the bonding around the metal centres are eclipsed, however with the POCOP ligands at approximately 90° to one another, presumably this results in minimising the steric clash between the *tert*-butyl groups. The DFT-optimised geometry of **8** is in good agreement with its experimental counterpart, although the BP86 functional somewhat underestimates the Ti–Ti separation. A survey of different functionals reveals that this trend is general for *meta*-GGA and GGA functionals, whilst hybrid functionals tend to give Ti–Ti distances closer to the experimental value. Nonetheless, the calculations support the assignment of two bridging hydrides in the structure of **8**, with other isomers being energetically disfavoured (see Fig. S49 and S50†). In the computed triplet electronic ground state of **8**, stabilised relative to the antiferromagnetically coupled singlet diradical by ~1 kcal mol⁻¹, one unpaired electron is centred on each Ti ion.

^{1}H NMR studies of the reaction mixture at 5 °C showed formation of neopentane and a broad resonance at a chemical shift of −0.52 ppm which is assigned to the Ti–(μ-H)–Ti

environment, as upon reaction with deuterium gas this resonance is absent. **8**, like **1**, **6** and **7**, gives a triplet in its X band CW EPR spectrum at room temperature (see ESI, Fig. S6†). The principle resonance comes at a coincident g_{iso} value as the other examples measured, with coupling to two phosphorus resonances. This implies the electron is localised onto the titanium centre and there is no bonding interaction between the metal centres. The effective magnetic moment (measured by Evan's method) is $3.37\mu_B$. This is somewhat higher than the ideal spin-only value for two electrons.

Conclusion

The ^{R}POCOP ligand framework has been successfully deployed onto titanium. Both (^{R}POCOP)Ti(III) and (^{R}POCOP)Ti(IV) complexes can be made, and different substituents on the POCOP ligand can be used. For Ti(IV), using the bulky ^{tBu}POCOP ligand results in monomeric species **2** to be formed whereas changing the ligand for the slightly smaller ^{iPr}POCOP allows for dimerization (**4**). Interestingly in the presence of THF, Ti(IV) and [^{tBu}POCOP]Li reacts in an unprecedented rearrangement of the POCOP ligand. Such a rearrangement does not occur when Ti(III) is used. (^{tBu}POCOP)TiCl$_2$, **1**, can be made on the gram-scale and can be easily derivatised with alkylating and arylating reagents. All of these species have been well-characterised including using X-ray crystallography and EPR.

The neopentyl compound (^{tBu}POCOP)TiNpCl, **7**, was reacted with H_2, demonstrating the ability of the POCOP ligand to stay attached even in reactive condition. This resulted in the formation of a rare titanium chlorohydride complex, which is remarkably stable under an inert atmosphere. Overall this opens the door to using this valuable and easily customisable ligand platform, the fundamental pincer ligand, with early transition metals.

Conflicts of interest

The authors declare there are no conflicts of interest.

Acknowledgements

References

1 C. J. Moulton and B. L. Shaw, *J. Chem. Soc., Dalton Trans.*, 1976, 1020–1024.

2 E. Peris and R. H. Crabtree, *Chem. Soc. Rev.*, 2018, **47**, 1959–1968.

3 G. van Koten and R. A. Gossage, *The Privileged pincer-metal platform: Coordination chemistry & applications*, Springer International Publishing, 2015.

4 L. Alig, M. Fritz and S. Schneider, *Chem. Rev.*, 2019, **119**, 2681–2751.

5 A. Kumar, T. M. Bhatti and A. S. Goldman, *Chem. Rev.*, 2017, **117**, 12357–12384.

6 R. Shi, Z. Zhang and X. Hu, *Acc. Chem. Res.*, 2019, **52**, 1471–1483.

7 J. I. van der Vlugt, *Eur. J. Inorg. Chem.*, 2012, **2012**, 363–375.

8 D. M. Roddick, in *Organometallic Pincer Chemistry*, ed. G. van Koten and D. Milstein, Springer-Verlag, Berlin, 1st edn, 2013, pp. 49–88.

9 A. S. Goldman, A. H. Roy, Z. Huang, R. Ahuja, W. Schinski and M. Brookhart, *Science*, 2006, **312**, 257–261.

10 Z. Huang, P. S. White and M. Brookhart, *Nature*, 2010, **465**, 598–601.

11 D. Himmelbauer, B. Stöger, L. F. Veiros, M. Pignitter and K. Kirchner, *Organometallics*, 2019, **38**, 4669–4678.

12 J. Zhang, W. Huang, K. Han, G. Song and S. Hu, *Dalton Trans.*, 2022, **51**, 12250–12257.

13 P. Chirik and R. Morris, *Acc. Chem. Res.*, 2015, **48**, 2495.

14 R. J. Burford, A. Yeo and M. D. Fryzuk, *Coord. Chem. Rev.*, 2017, **334**, 84–99.

15 B. C. Bailey, J. C. Huffman, D. J. Mindiola, W. Weng and O. V. Ozerov, *Organometallics*, 2005, **24**, 1390–1393.

16 C. M. Brammell, E. J. Pelton, C. H. Chen, A. A. Yakovenko, W. Weng, B. M. Foxman and O. V. Ozerov, *J. Organomet. Chem.*, 2011, **696**, 4132–4137.

17 S. S. Nadif, M. E. O'Reilly, I. Ghiviriga, K. A. Abboud and A. S. Veige, *Angew. Chem., Int. Ed.*, 2015, **54**, 15138–15142.

18 Y. Sekiguchi, F. Meng, H. Tanaka, A. Eizawa, K. Arashiba, K. Nakajima, K. Yoshizawa and Y. Nishibayashi, *Dalton Trans.*, 2018, **47**, 11322–11326.

19 Z. Mo, T. Shima and Z. Hou, *Angew. Chem., Int. Ed.*, 2020, **59**, 8635–8644.

20 S. Dey and T. K. Hollis, *Inorganics*, 2021, **9**, 15.

21 P. Zatsepin, E. Lee, J. Gu, M. R. Gau, P. J. Carroll, M. H. Baik and D. J. Mindiola, *J. Am. Chem. Soc.*, 2020, **142**, 10143–10152.

22 T. Kurogi, J. Won, B. Park, O. S. Trofymchuk, P. J. Carroll, M. H. Baik and D. J. Mindiola, *Chem. Sci.*, 2018, **9**, 3376–3385.

23 D. P. Solowey, M. V. Mane, T. Kurogi, P. J. Carroll, B. C. Manor, M. H. Baik and D. J. Mindiola, *Nat. Chem.*, 2017, **9**, 1126–1132.

24 T. Kurogi, B. Pinter and D. J. Mindiola, *Organometallics*, 2018, **37**, 3385–3388.

25 T. Shima, S. Hu, G. Luo, X. Kang, Y. Luo and Z. Hou, *Science*, 2013, **340**, 1549–1552.

26 B. Wang, G. Luo, M. Nishiura, S. Hu, T. Shima, Y. Luo and Z. Hou, *J. Am. Chem. Soc.*, 2017, **139**, 1818–1821.

27 K. Ma, W. E. Piers and M. Parvez, *J. Am. Chem. Soc.*, 2006, **128**, 3303–3312.

28 J. Gordon, S. Hildebrandt, K. R. Dewese, S. Klare, A. Gansäuer, T. V. RajanBabu and W. A. Nugent, *Organometallics*, 2018, **37**, 4801–4809.

29 N. Tsoureas, J. C. Green and F. G. N. Cloke, *Dalton Trans.*, 2018, **47**, 14531–14539.

30 E. G. Perevalova, I. F. Urazowski, D. A. Lemenovskii, Y. L. Slovokhotov and Y. T. Struchkov, *J. Organomet. Chem.*, 1985, **289**, 319–329.

31 T. J. Hebden, R. R. Schrock, M. K. Takase and P. Müller, *Chem. Commun.*, 2012, **48**, 1851–1853.

32 T. J. Hebden, A. J. St. John, D. G. Gusev, W. Kaminsky, K. I. Goldberg and D. M. Heinekey, *Angew. Chem., Int. Ed.*, 2011, **50**, 1873–1876.

33 H. J. Reich, *Chem. Rev.*, 2013, **113**, 7130–7178.

34 J. S. Ritch, D. Julienne, S. R. Rybchinski, K. S. Brockman, K. R. D. Johnson and P. G. Hayes, *Dalton Trans.*, 2014, **43**, 267–276.

35 A. Pape, M. Lutz and G. Müller, *Angew. Chem., Int. Ed. Engl.*, 1994, **33**, 2281–2284.

36 C. Idelson, L. Webster, T. Krämer and F. M. Chadwick, *Dalton Trans.*, 2020, **49**, 16653–16656.

37 I. Göttker-Schnetmann, P. White and M. Brookhart, *J. Am. Chem. Soc.*, 2004, **126**, 1804–1811.

38 N. Serpone, P. H. Bird, D. G. Bickley and D. W. Thompson, *J. Chem. Soc., Chem. Commun.*, 1972, 217–218.

39 A. W. Addison, T. N. Rao, J. Reedijk, J. Van Rijn and G. C. Verschoor, *J. Chem. Soc., Dalton Trans.*, 1984, 1349–1356.

40 N. Rahimi, B. de Bruin and P. H. M. Budzelaar, *Organometallics*, 2017, **36**, 3189–3198.

41 P. L. A. Popelier and G. Logothetis, *J. Organomet. Chem.*, 1998, **555**, 101–111.

42 W. Scherer and G. S. McGrady, *Angew. Chem., Int. Ed.*, 2004, **43**, 1782–1806.

43 R. H. Duncan Lyngdoh, H. F. Schaefer and R. B. King, *Chem. Rev.*, 2018, **118**, 11626–11706.